Atmospheric
Chemistry
and Physics

Measurement of light-absorbing particles in surface snow of central and western Himalayan glaciers: spatial variability, radiative impacts, and potential source regions

Chaman Gul[1,2,3,4], **Shichang Kang**[1,4], **Siva Praveen Puppala**[2], **Xiaokang Wu**[5], **Cenlin He**[6], **Yangyang Xu**[5], **Inka Koch**[2,7], **Sher Muhammad**[2], **Rajesh Kumar**[6], and **Getachew Dubache**[3]

[1]State Key Laboratory of Cryosphere Sciences, Northwest Institute of Eco-Environment and Resources, Chinese Academy of Sciences, Lanzhou 73000, China
[2]International Centre for Integrated Mountain Development (ICIMOD), G.P.O. Box 3226, Kathmandu, Nepal
[3]Reading Academy, Nanjing University of Information Science and Technology, 219 Ningliu Road, Nanjing, Jiangsu 210044, China
[4]University of Chinese Academy of Sciences, Beijing, China
[5]Department of Atmospheric Sciences, Texas A&M University, College Station, TX 77843, USA
[6]Research Applications Laboratory, National Center for Atmospheric Research, Boulder, CO 80301, USA
[7]Department of Geosciences, University of Tübingen, Schnarrenbergstr. 94–96, 72076 Tübingen, Germany

Correspondence: Siva Praveen Puppala (sivapraveen.puppala@icimod.org) and Chaman Gul (gulchamangul76@yahoo.com)

Abstract. We collected surface snow samples from three different glaciers – Yala, Thana, and Sachin – in the central and western Himalayas to understand the spatial variability and radiative impacts of light-absorbing particles. The Yala and Thana glaciers in Nepal and Bhutan, respectively, were selected to represent the central Himalayas. The Sachin glacier in Pakistan was selected to represent the western Himalayas. The samples were collected during the pre- and post-monsoon seasons of the year 2016. The samples were analyzed for black carbon (BC) and water-insoluble organic carbon (OC) through the thermal optical method. The average mass concentrations (BC $2381\,\mathrm{ng\,g^{-1}}$; OC $3896\,\mathrm{ng\,g^{-1}}$; dust $101\,\mathrm{\mu g\,g^{-1}}$) in the western Himalayas (Sachin glacier) were quite high compared to the mass concentrations (BC $358\,\mathrm{ng\,g^{-1}}$, OC $904\,\mathrm{ng\,g^{-1}}$, dust $22\,\mathrm{\mu g\,g^{-1}}$) in the central Himalayas (Yala glacier). The difference in mass concentration may be due to the difference in elevation, snow age, local pollution sources, and meteorological conditions. BC in surface snow was also estimated through Weather Research and Forecasting (WRF) model coupled with Chemistry (WRF-Chem) simulations at the three glacier sites during the sampling periods. Simulations reasonably capture the spatial and seasonal patterns of the observed BC in snow but with a relatively smaller magnitude. Absolute snow albedo was estimated through the Snow, Ice, and Aerosol Radiative (SNICAR) model. The absolute snow albedo reduction ranged from 0.48 % (Thana glacier during September) to 24 % (Sachin glacier during May) due to BC and 0.13 % (Yala glacier during September) to 5 % (Sachin glacier during May) due to dust. The instantaneous radiative forcing due to BC and dust was estimated in the range of 0 to 96.48 and 0 to $25\,\mathrm{W\,m^{-2}}$, respectively. The lowest and highest albedo reduction and radiative forcing were observed in central and western Himalayan glaciers, respectively. The potential source regions of the deposited pollutants were inferred using WRF-Chem tagged-tracer simulations. Selected glaciers in the western Himalayas were mostly affected by long-range transport from the Middle East and central Asia; however, the central Himalayan glaciers were mainly affected by local and south

Asia emissions (from Nepal, India, and China) especially during the pre-monsoon season. Overall, south Asia and west Asia were the main contributing source regions of pollutants.

1 Introduction

Black carbon (BC) is a distinct type of carbonaceous material that is formed primarily in flames. BC particles in the atmosphere are generally produced by the incomplete combustion of fossil fuel, biofuel, and biomass. BC is only a minor contributor to aerosol mass but has great climatic interest as a strong absorber of solar radiation (Quinn et al., 2008; Ramanathan and Carmichael, 2008). In addition to warming, BC particles can interact with clouds, changing their microphysical properties and thus impacting the climate (Wang et al., 2018; Bond et al., 2013). Besides this, several studies in the past have highlighted the role of BC in the cryosphere (Kang et al., 2019, 2020).

The cryosphere is one of the most sensitive indicators of climate change. The temperature rise in cryospheric regions is generally larger than that in other regions on the global scale (Pepin and Lundquist, 2008; Kang et al., 2010; You et al., 2021). BC particles are deposited on the glaciers or snow cover surface, decreasing the surface albedo and absorbing more solar radiation (Warren and Brandt, 2008; He et al., 2017), which accelerates snowmelt and ice melt and triggers albedo feedback (Flanner et al., 2009; Hansen and Nazarenko, 2004; Kang et al., 2020). The forcing produced by BC and other light-absorbing particles (LAPs) further affects the regional climate (Flanner et al., 2009; Ji et al., 2015) and leads to complex responses of the Earth's climate system (Hansen et al., 1997). The largest climate forcing from BC in the snow is estimated to occur over the Tibetan Plateau (TP) and Himalayas (Flanner et al., 2009; Ji et al., 2015).

Mountain glaciers are the most important freshwater resources to the inhabitants of arid and semi-arid regions (Hock, 2005; Mayer et al., 2006). The Himalayas is considered the world's largest freshwater reservoir outside the polar regions (Immerzeel et al., 2010; Marcovecchio et al., 2021). The economy and lives of millions of people in the region are influenced by the changes in mountain river discharge downstream of the Himalayas (Vaux et al., 2012). Lack of in situ data, the low resolution of emission inventories, and coarse model resolutions prevent an accurate evaluation of LAP impacts on snow albedo and radiative forcing. Many glaciers have retreated in the region due to climate warming (Zhang et al., 2009; Kang et al., 2010; Yao et al., 2019) and possibly due to LAP-induced surface darkening (Flanner et al., 2009; Qian et al., 2011; Kang et al., 2019). Glacier retreat in the TP and the Himalayan region has serious consequences because snow and runoff from this region are sources of major rivers in Asia, and the availability of freshwater resources has profound effects on human health and agriculture (Immerzeel et al., 2010). However, large uncertainties remain regarding glacier retreat driven predominately by the deposition of BC and other LAPs (Bolch et al., 2012; Kang et al., 2020).

Snow albedo is an important indicator of the surface energy budget over a snow-covered area. Small changes in surface snow albedo can have large impacts on surface warming due to the rapid feedback involving changes to sublimation, snow morphology, and melt rates (Bond et al., 2013). The concentration of LAPs in surface snow is a major factor that affects snow albedo. BC and other LAPs present in the snow reduce the albedo in the visible portion of the electromagnetic spectrum (Flanner et al., 2007). Besides the concentration of pollutants deposited on the surface of the snow, multiple other factors, such as the solar zenith angle (SZA), snow grain size, snow grain shape, snow surface texture, snow density, and snowpack thickness, can also affect snow albedo (He and Flanner, 2020). The radiative transfer model used for the albedo has brought a better understanding of snow optical properties in the shortwave spectrum (He and Flanner, 2020; Tripathee et al., 2021). We estimated the spectral snow albedo using the online Snow, Ice, and Aerosol Radiative (SNICAR) model (Flanner and Zender, 2006). The model was originally developed by Flanner et al. (2007), was further updated by He et al. (2018) and Dang et al. (2019), and has been widely used in simulating the impacts of LAPs on snow albedos (Qu et al., 2014).

Here we present the mass concentration of BC, water-insoluble organic carbon (OC), and mineral dust in surface snow from the ablation and accumulation zones of selected glaciers, located in three different countries (Nepal, Bhutan, and Pakistan) on the southern slope of the Himalayas. The Yala and Thana glaciers were selected from the central Himalayas, while the Sachin glacier was selected from the western Himalayas. To reasonably compare the results (mass concentrations and optical and radiative properties) across the central and western Himalayas, samples were collected on similar dates of the same seasons (pre-monsoon and post-monsoon). We investigate the spatial variability in BC, OC, and mineral dust concentrations due to differences in the source region, meteorology, deposition, and post-deposition processes. The measured mass concentrations were compared to regional model simulations. The associated changes in surface snow albedo and radiative forcing (RF) by mineral dust and BC in surface snow were estimated using the SNICAR model. We also aim to identify the potential source regions of pollution reaching sampling sites using tracer-tagged model simulations.

Table 1. Snow sampling time and locations from selected glaciers.

Glacier	Lat, long	Sampling date	Average elevation	Himalayas
Yala (Nepal)	28°14′12.25″ N, 85°37′04.24″ E	4–7 May 2016	4950 m	Central
Yala (Nepal)	28°14′12.25″ N, 85°37′04.24″ E	29 September 2016	4950 m	Central
Thana (Bhutan)	28°01′22.23″ N, 90°36′28.72″ E	15 September 2016	5400 m	Central
Sachin (Pakistan)	35°19′55″ N, 74°45′35″ E	15 May 2016	3230 m	Western

2 Study area and meteorology

Samples were collected from the Yala glacier (28°14′ N, 85°37′ E) in the Langtang Valley of Nepal, the Thana glacier (28°01′ N, 90°36′ E) in the Chamkhar Valley of Bhutan, and the Sachin glacier (35°19′ N, 74°45′ E) in northern Pakistan (Table 1). Monthly mean surface air temperature and precipitation (reanalysis data) over the selected glaciers were analyzed and compared for the western and central Himalayan glaciers from April 2015 to October 2017 (Table 2). The Yala glacier is a plateau-shaped glacier that has an elevation range between 5160 and 5750 m a.s.l. The length of the Yala glacier is 1.5 km facing the northwest. The glacier is located away from the residential area and is mostly covered by snow, especially during the winter season. Details about the metrological conditions at the Yala glacier are available in Rai et al. (2019) and Gul et al. (2021). The Thana glacier is a gently sloping glacier with slight debris cover and an elevation range between 5250 and 5700 m a.s.l. The length of the glacier is about 5 km, facing the southwest. The Thana glacier is mostly covered by fresh snow, especially during the winter season. The Sachin glacier has a gentle slope with dense debris cover in its ablation area with an altitude range from 3105 to 4976 m a.s.l. The length of the Sachin glacier is around 8 km facing northeast. In general, the Sachin glacier is a low-elevation and relatively debris-covered glacier compared to the central Himalayan glaciers (Yala and Thana). Precipitation in the central Himalayan glaciers (Yala and Thana) was higher than that of the western Himalayan glacier (Sachin), especially from April to October each year (Table 2). Surface air temperature over the Yala and Sachin glaciers was higher than that of the Thana glacier. The geographical location of the selected glaciers and snow sampling locations are shown in Fig. 1. Besides the difference in altitude, latitude, and meteorology of the selected glaciers in the central and western Himalayas, there is also a difference in the surface conditions shown in Fig. S1 in the Supplement.

3 Methodologies

3.1 Snow sampling and analysis

Surface snow samples were collected from the central and western Himalayan glaciers during May and September 2016. Samples were taken from the ablation and accumulation zones of the selected glaciers; however, a few snow samples were also collected from the surrounding nearby areas of the Yala and Sachin glaciers. The Sachin glacier samples were of relatively aged snow and had less snow thickness as compared to the samples collected from the Thana and Yala glaciers (Fig. S1). At each sampling location, Whirl-Pak bags were used to collect samples from the upper 0–10 cm of depth (approximately 2 L, unmelted). The samples were kept frozen until they were melted and filtered in through the quartz filters near the sampling site. The snow density was measured with a small density kit. The snow grain size was measured through a hand lens (25×) with an accuracy of 0.02 mm. The same sampling protocol was used for all three selected glaciers. A detailed description of the sampling procedure is described in Y. Li et al. (2016). Quartz filters were used to measure the mass concentration of BC, OC, and dust in the collected samples. BC and OC present in snow samples were analyzed by a filter-based thermal–optical analysis method using a DRI® Model 2005 analyzer (Chow et al., 1993). Filters were analyzed at the State Key Laboratory of Cryosphere Sciences, Northwest Institute of Eco-Environment and Resources, Chinese Academy of Sciences. Before starting the analysis, a piece of the sampled filters was put in an oven for a few minutes to eliminate the water vapor content and volatile organic compounds. Further detailed information on the instrument and analysis method can be referred to in earlier studies (Gul et al., 2018).

3.2 Estimation of snow albedo reduction and radiative forcing

The online snow simulation model SNICAR (Flanner et al., 2007, http://snow.engin.umich.edu/, last access: 20 April 2022) was used to estimate snow albedo calculation for the collected samples. The model has been used by multiple studies in the past (Gul et al., 2018; Zhang et al., 2018). Albedo was simulated based on an hourly SZA at the sampling site with an averaged mass concentration of BC, dust, and other input parameters such as snow grain size, snow density, and snow depth from measurements. We computed broadband snow albedo for direct solar incident radiation under mid-latitude, winter, clear-sky conditions (Table S1 in the Supplement). Depending on geographical location, 10 to 15 SZAs were used (between 0 and 90°) during instantaneous daytime albedo simulation. Albedo was simulated in four categories: (1) broadband albedo with BC and
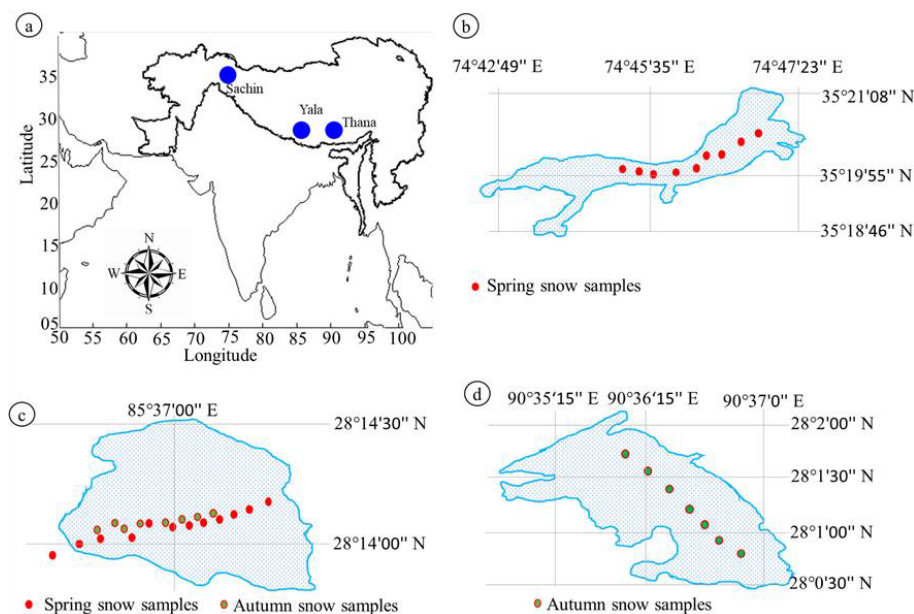
Figure 1. Study area map. **(a)** Locations of selected glaciers in the Himalayan Karakoram and Hindu Kush region. **(b)** The Sachin glacier in Pakistan. **(c)** The Yala glacier in Nepal. **(d)** The Thana glacier in Bhutan.

dust in snow; (2) broadband albedo with BC in snow only; (3) broadband albedo with dust in snow only; and (4) broadband albedo with the absence of BC and dust, which was considered a reference albedo. Radiative implications caused by snow darkening due to BC and dust deposition were investigated using the albedo reduction and the radiative transfer model Santa Barbara DISORT Atmospheric Radiative Transfer (SBDART) (Ricchiazzi et al., 1998). To evaluate the amount of additional solar radiation absorbed by the snow in the presence of BC and dust, we estimated the mean solar irradiance and its characteristics via SBDART, which has been used in the past (Yang et al., 2015). According to the location of the sampling site, the characteristics of the atmospheric profiles such as water vapor, aerosols, or ozone were set in the model. RF for the snow samples was estimated by following Eq. (1):

$$\text{RF}_x = R_{\text{in-short}} \times \Delta\alpha_x , \tag{1}$$

where $R_{\text{in-short}}$ denotes incident shortwave solar radiation for selected SZA and $\Delta\alpha_x$ denotes the reduction in albedo due to BC, dust, or both, as simulated by the SNICAR model.

3.3 Potential source region of pollutants

Glaciers of the Himalayan Karakoram and Hindu Kush (HKH) region are located at high altitudes as compared to the sources of the major pollutants. LAPs including BC and dust can be transported from urban areas towards glaciated areas (Yasunari et al., 2010; Kang et al., 2019). Multiple approaches, including climate circulation modeling, combinations of bottom-up inventories, and back air trajectories, have

been used in the past to determine the possible source regions of pollution in the HKH region. To identify the potential source region of pollution arriving at the observation sites, we used the Weather Research and Forecasting (WRF) model coupled with Chemistry (WRF-Chem version 3.9.1.1) simulations (Grell et al., 2005). The model uses region-tagged tracers for different regions across the world.

WRF-Chem simulations were used to estimate BC mass concentration in surface snow and deposition of BC particles on three selected glaciers (Yala, Thana, and Sachin). We archived the hourly model results for instantaneous BC deposition and concentration in snow. The horizontal grid spacing of the model was $20 \, \text{km} \times 20 \, \text{km}$ with 35 vertical levels stretching from the surface up to 50 hPa ($\sim 20 \, \text{km}$). The updated Model for Ozone And Related chemical Tracers (MOZART) was applied for the gas-phase chemistry (Knote et al., 2014), while aerosols in the WRF-Chem were simulated via the Model for Simulating Aerosol Interactions and Chemistry (MOSAIC) (Zaveri et al., 2008). We use the Global Data Assimilation System (GDAS) from the National Centers for Environmental Prediction (NCEP) for the meteorological initial and boundary conditions. We used the Fire INventory from NCAR (FINN; NCAR is the National Center for Atmospheric Research), Emission Database for Global Atmospheric Research developed for Hemispheric Transport of Air Pollution (EDGAR-HTAP), and MEGAN (Model of Emissions of Gases and Aerosols from Nature) for biomass burning emissions, anthropogenic emissions, and online biogenic emissions, respectively. For chemical boundary conditions, we used the NCAR global CAM-chem simulation dataset (https://rda.ucar.edu/datasets/ds313.7/, last access: 22

Table 2. Comparison of BC mass concentration, albedo reduction, radiative forcing, and potential source regions of pollutants for central and western Himalayan glaciers during the study period.

	Central Himalayas min to max (average)	Western Himalayas min to max (average)	Time period
Monthly mean temperature (°C)	2.05 to 14.36 (10.35) Yala −9.11 to 5.68 (0.23) Thana	−10.78 to 14.63 (3.57) Sachin	April 2015–October 2017
Monthly mean precipitation (mm d^{-1})	0.04536 to 41.472 Yala 1.0195 to 50.112 Thana	0.1546 to 5.866 (Sachin)	April 2015–October 2017
Monthly mean precipitation (mm), during sampling months	(4) Yala + Thana (29) Yala + Thana	(4) Sachin (3) Sachin	April 2016 September 2016
Elevation of sampling location (m)	4580 to 5675 (5127)	3134 to 3957 (3545)	
Observed BC in surface snow (ng g^{-1})	21 to 2529 ($\sim$ 350)	835 to 3545 ($\sim$ 2300)	2016
Albedo reduction (%) due to BC particles in snow	0.13 to 3.82	12.00 to 24.00	2016
Instantaneous radiative forcing (W m^{-2}) due to BC particles	0.0 to 39.65	0.03 to 96.48	2016
Potential source regions of pollutants			
WRF-Chem simulations	For the Yala site, it is dominated (>50 %) by anthropogenic emissions from India and Nepal for both May and October, while the biomass burning contribution (>20 %) increases largely in May. For the Thana site, it is dominated (>60 %) by anthropogenic emissions from China and India in September, while anthropogenic emissions from Bhutan and Myanmar each contribute about 10 %.	For the Sachin site, it is predominantly affected by anthropogenic emissions from India and Pakistan (total contribution >80 %), while the spring biomass burning only contributes $\sim$ 10 % in May.	

June 2022). Key meteorological variables such as winds, temperature, and water vapor above the planetary boundary layer (PBL) were nudged every 6 h towards the NCEP GDAS reanalysis fields to reduce temporal error growth in meteorological variables. We used the Community Land Model (CLM) scheme for the land component in WRF-Chem. The CLM can simulate BC concentration in snowpack and its effects on snow albedo (Flanner et al., 2007). We used online coupled BC deposition fluxes from the atmosphere component of WRF-Chem with the CLM following Zhao et al. (2014). We also implemented a tagged-tracer method (Kumar et al., 2015) to track anthropogenic BC emissions from 10 different Asian countries surrounding the TP areas, as well as BC emissions from Asian biomass burning and the domain boundary (i.e., areas outside Asia). The 10 tracked anthropogenic emission source regions include China, India, Nepal, Pakistan, Afghanistan, Bhutan, Bangladesh, Myanmar, southeast Asia, and the rest of Asia.

The aim of the model simulation was to estimate the BC mass concentration in surface snow, deposition of BC particles, and the source contribution to BC deposition on snow.

4 Results and discussions

4.1 Concentrations of light-absorbing particles in surface snow

The average mass concentration of LAPs in surface snow of the Yala glacier was 358 ng g^{-1} for BC, 904 ng g^{-1} for OC, and 22 µg g^{-1} for dust in spring (May), and there were relatively low concentrations of 69 ng g^{-1} for BC, 177 ng g^{-1} for OC, and 4 ng g^{-1} for dust during autumn (September). These mass concentrations of BC and OC in surface snow were comparable to the study result conducted on the Yala glacier in May 2017 (Gul et al., 2021).

High LAP concentration in the pre-monsoon is due to an effective transport mechanism from the Indian subcontinent

and an additional source such as forest fires (Gul et al., 2021). The average surface concentrations of BC, OC, and dust in the Thana glacier samples during the autumn season were 39, 115 ng g^{-1}, and 34 µg g^{-1}, respectively. Possible reasons for the lower concentration at the Thana glacier may be due to the relatively high elevation of the sampling location and relatively fresh snow. A strong effect of LAPs (BC and dust) has been observed at lower elevations in comparison to higher elevations (Li et al., 2017). The average concentrations of BC, OC, and dust measured in the selected western Himalayan glacier (Sachin) during May were 2381, 3896, and 101 ng g^{-1}, respectively, and were relatively high during October with values of 5314 ng g^{-1} for BC and 546 µg g^{-1} for dust (Gul et al., 2018). The observed average mass concentrations in the western Himalayas were higher than those in the central Himalayas. The BC mass concentration difference might be due to the difference in snow type, precipitation rate, local emission, the elevation of sampling sites, meteorology, and BC deposition over the glacier surfaces. Post-monsoon dry deposition of LAPs over the surface of the snow was an important factor. The pollutant source regions for the central and western Himalayas are different. In the case of the central Himalayas, pollutants emitted during pre-monsoon convection and multiple forest fire events are effectively lifting and transported towards the central Himalayan glaciers. Due to strong inversion in winter, most of the pollutants become stuck near the surface, whereas in the monsoon, pollutants are scavenged by rain. Thus the pre-monsoon is a very significant period in the transport process in the central Himalayas. Snow samples collected from the western side of the Himalayas were aged as compared to the central part; post-deposition ion (or enrichment) of LAPs over the snow surface increased the concentration in the snow (Kang et al., 2019). The majority of the samples from the western Himalayan side were from ablation zones of the glacier, where concentrations of LAPs are higher as compared to the accumulation zone of the glacier. Li et al. (2017) showed a strong negative relationship between the elevation of glacier sampling locations and the concentration of LAPs. Therefore strong melting of surface snow and ice in the glacier ablation zone could lead to BC enrichment, which causes high BC concentrations (Li et al., 2017). In the case of western Himalayan glacier sites, snow samples were collected long after the snowfall and the concentration of pollutants would also have increased in the surface snow due to dry deposition. The surface concentrations of the individual samples collected from the Yala, Thana, and Sachin glaciers during May and September 2016 are shown in Fig. 2 and Table S2. BC and OC concentrations on our selected glaciers with a comparison to other glaciers of the TP and the surrounding region are shown in Fig. 3 and Table S3. It was observed that the concentrations of BC, OC, and dust in the central Himalayan glaciers (Yala and Thana) were comparable to other reported results. In the past, similarly high concentrations were reported in the region such as the Tian Shan (Tibetan) glacier
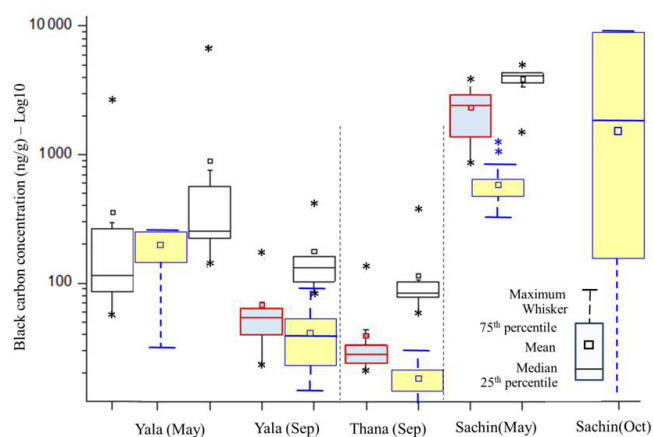

Figure 2. Box-and-whisker plots of black carbon (red box) and organic carbon (black box) concentrations (ng g^{-1}) in snow samples collected from three different glaciers in spring and autumn 2016. The yellow boxes represent BC content in surface snow from WRF-Chem simulations. Stars (*) represent outliers.

(Xu et al., 2012); Qilian Mountains, northeastern TP (Y. Li et al., 2016); northeastern China (Wang et al., 2017); southeastern TP (Niu et al., 2020; Zhang et al., 2017); central Asian glaciers (Schmale et al., 2017); and Tian Shan (Kang et al., 2020).

The yellow boxes of Fig. 2 show the WRF-Chem-modeled BC concentrations in surface snow at the three measurement glacier sites during the measurement periods. Compared to the observations shown with red boxes in Fig. 2, model results reasonably capture the spatial and seasonal patterns and variables of the observed BC in the snow with a relatively small magnitude. The modeled variation at the Sachin site during the October sampling periods is much larger than that of the observations (Gul et al., 2018). The discrepancies between model results and observations are due to model uncertainties from (1) the relatively coarse grid spacing that may not capture the transport over the complex TP terrain, (2) the underestimated anthropogenic emissions that are not representative of the measurement periods, and (3) deficiencies in model physical parameterizations that affects BC transport and deposition. The WRF-Chem model implicitly accounts for the surface impurity enrichment during snow ablation by using a low meltwater scavenging efficiency for BC. However, we notice that this meltwater scavenging efficiency parameter could be associated with large uncertainties (Qian et al., 2014) due to the lack of direct observational constraints. We also note that the observed variation at each site shown in Fig. 2 includes both the temporal and the subgrid variabilities derived from multiple sampling locations surrounding each site (Fig. 1). In contrast, all the measurement locations at each particular glacier site are located within a single model grid. As a result, the model is unable to resolve this subgrid information and hence only includes the temporal variability for each selected site.
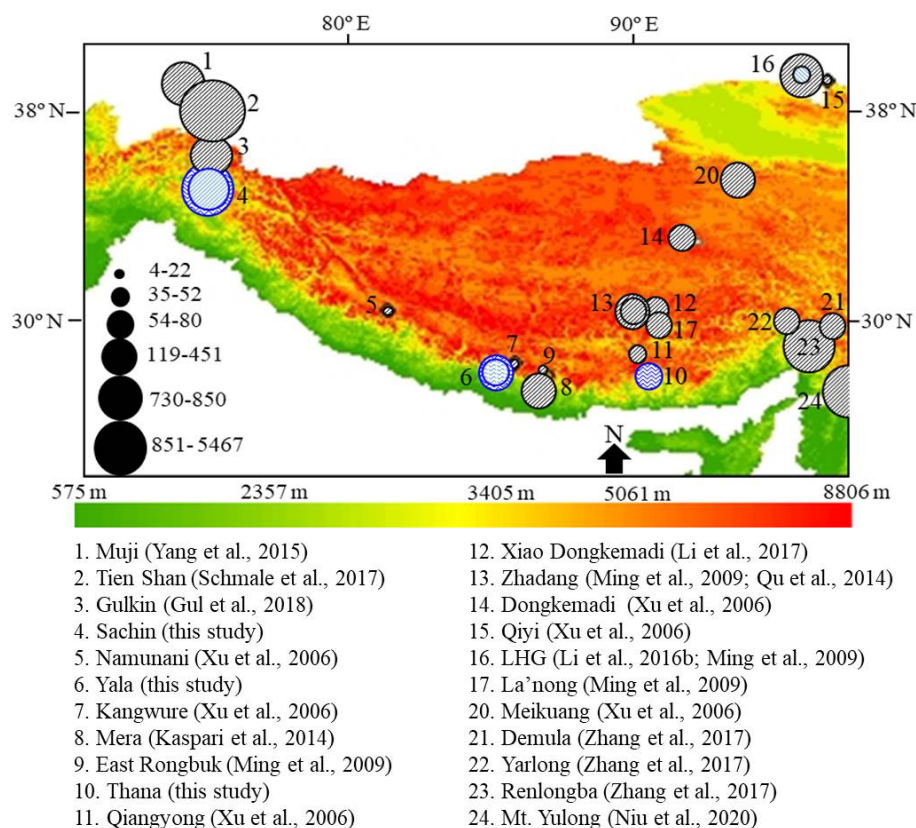
Figure 3. Black carbon concentrations ($ng\,g^{-1}$) in snow/ice samples in the Himalayas, Karakoram, and Tibetan Plateau in previous studies (black circles) and this study (blue circles).

4.2 Surface snow albedo and radiative forcing

The minimum daytime absolute albedo reduction due to combined BC and dust, BC only, and dust only was in the range of 1.03 %–13.44 %, 0.48 %–12.42 %, and 0.12 %–2.12 %, respectively. The maximum daytime albedo reduction due to combined BC and dust, BC only, and dust only was in the range of 1.98 %–24.97 %, 1.05 %–24 %, and 0.25 %–4.8 %, respectively. The lowest and highest contributions in albedo reduction were observed in the central Himalayas (September) and the western Himalayas (May), respectively. Snow albedo reduction (%) derived from samples collected from the Yala glacier (during May 2016) and the Thana glacier (during September 2016) was in the range of 0.13 %–3.82 % and 0.90 %–1.99 %, respectively. A significant difference in daytime albedo reduction between the western and central Himalayas was mainly due to the difference in mass concentrations of pollutants and snow age. The pollutant concentrations in the western Himalayan samples (Sachin glacier) were higher, resulting in higher albedo reduction as compared to the central Himalayan (Yala and Thana glaciers) samples. The average elevation difference between central and western sampling sites was greater than 1000 m, where a high concentration of pollution is expected

at the low-elevation glacier of the western side as compared to the central part of the Himalayas. Snow samples collected in the central part of the Himalayas (Yala glacier) were much fresher as compared to the samples collected from the western side (Sachin glacier). Dust and other pollutants were visible over the surface of the Sachin glacier (Fig. S1). Aged snow had increased density, enlarged grain size, and increased concentration of BC and dust particles due to dry deposition on the snow surface. In the case of all sampling sites, the impact of BC on snow albedo reduction was greater than the impact of dust except at the Thana glacier, where the impact of dust was higher than that of BC (Fig. 4a). This may be due to a different dust type in Thana samples. Daytime snow albedo reductions (%) due to BC only, dust only, and both BC and dust are given in Fig. 4a.

The daytime instantaneous RF ($W\,m^{-2}$) ranged from 0.076 to 39.65 for the Yala glacier in May 2016, 0.006 to 18.26 for the Yala glacier in September 2016, 0.0 to 11.48 for the Thana glacier in September 2016, and 0.03 to 96.48 for the Sachin glacier during May 2016. RF for the western Himalayas (Sachin glacier) was quite high as compared to the central Himalayan glaciers (Yala and Thana glaciers). The radiative effect on the Sachin glacier was much more than that of other selected glaciers mainly due to low albedo
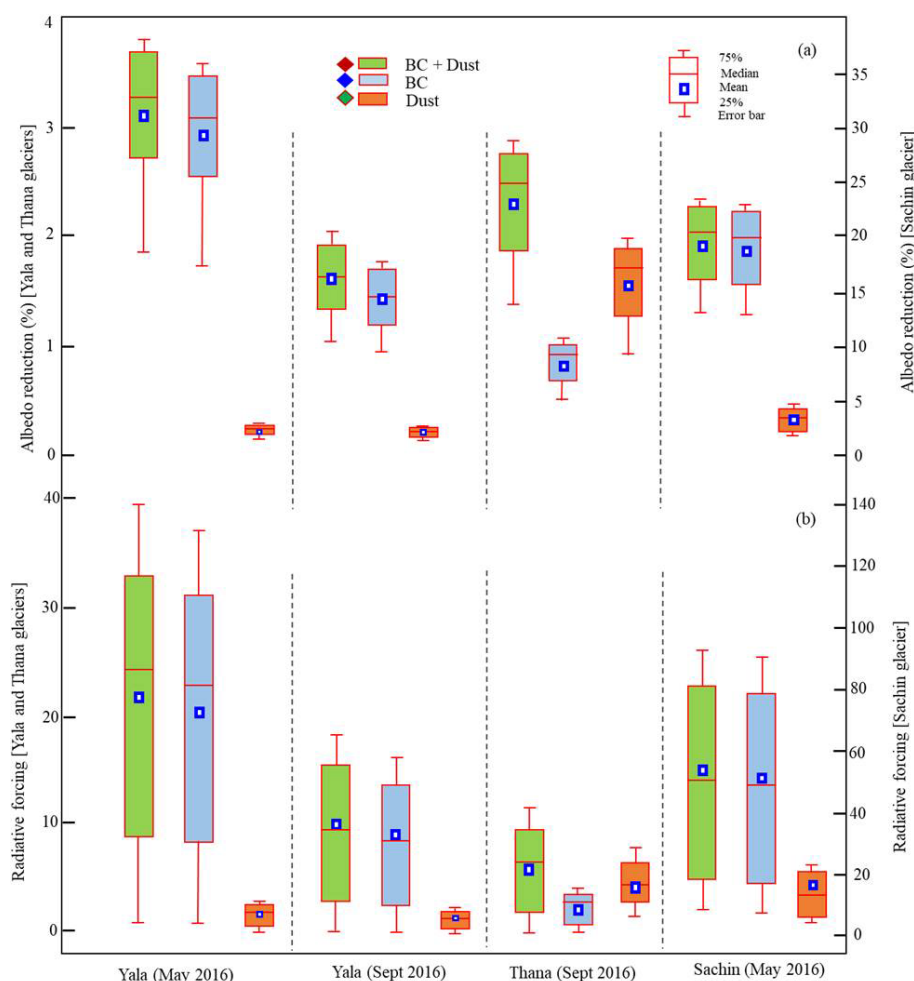
Figure 4. (a) Snow albedo reduction due to black carbon, dust, and combined black carbon and dust during the daytime for a range of solar zenith angles. **(b)** Average instantaneous radiative forcing based on albedo reduction values during the daytime.

and increased temperature. Zhang et al. (2017) reported that a reduction in albedo by 9 % to 64 % can increase the instantaneous RF by as much as 24.05–323.18 W m^{-2}. In the case of all sampling sites, the impact of BC on RF was greater than the impact of dust except at the Thana glacier, where the impact of dust was higher than that of BC (Fig. 4b). Therefore, BC can be a major pollutant in the snow responsible for reducing albedo and increasing warming in the selected glaciers. BC was the dominant factor in snowmelt in the Yala and Sachin glaciers; however, dust was the dominant factor in Thana glacier samples. According to Kaspari et al. (2014), RF caused by mineral dust was greater than that of dust. The BC and dust had low importance for RF in fresh snow (central Himalayas – Thana glacier) as compared to aged snow (western Himalayas – Sachin glacier). In the northern TP, BC played an important role in RF (C. Li et al., 2016), while in the central TP and Himalayas, dust was more important than BC (Kaspari et al., 2014). The average instantaneous RF caused by the combined contribution of BC and dust (BC +

dust), only BC, and only dust is shown in Fig. 4b as a function of surface snow types. Variation in the RF and albedo change for a particular pollutant type was due to variation in the SZA.

4.3 Potential source regions of pollutants

Figure 5 shows the contributions of different BC emission sources to the BC in snow from WRF-Chem tagged-tracer simulations. For the Yala site, it is dominated (> 50 %) by anthropogenic emissions from India and Nepal for both May and October, while the biomass burning contribution (> 20 %) increases largely in May primarily due to the spring burning activities in northern India (Kumar et al., 2011). In September, China's contribution also increases to > 20 % at Yala. For the Thana site, it is dominated (> 60 %) by anthropogenic emissions from China and India in September, while anthropogenic emissions from Bhutan and Myanmar each contribute about 10 %. The Sachin site is predominantly affected by anthropogenic emissions from India and Pakistan
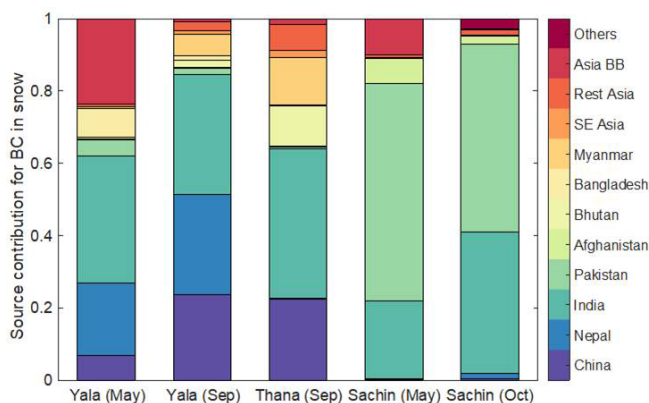
Figure 5. Source contributions to BC content in surface snow from WRF-Chem simulations at the three measurement glacier sites during the measurement periods. Source regions include anthropogenic emissions from China, India, Nepal, Pakistan, Afghanistan, Bhutan, Bangladesh, Myanmar, southeast (SE) Asia, and the rest of Asia, as well as Asian biomass burning (BB) and BC transported from areas outside the study domain ("Others").

(total contribution > 80 %), while the spring biomass burning only contributes > 10 % in May. Overall, the source contributions show large variation depending on the site locations and sampling seasons, but there is a consistent India contribution of 20 %–40 % across all the sites and seasons.

5 Discussion on uncertainty in measurements, albedo, and potential source identification of pollutants

The possible uncertainties in the present research were related to measurements, sampling, analysis, albedo, and RF estimation. When sampling at remote rural sites, sample preservation, filtration, and transport can modify the results if proper standard protocols are not followed. During laboratory analysis via thermal optical techniques, several uncertainties may be related to separating OC from BC in the sample (Gul et al., 2021). The level of generated uncertainty depended on the temperature protocol, sample type (residential cookstoves, diesel exhaust, rural aerosols, and urban aerosols), the amount of dust loading on the filter, and the analysis method. The overall accuracy in the measurement of OC, BC, and total carbon concentrations was estimated considering the mass contributions from field blanks and the analytical accuracy of concentration measurements. The uncertainty in the OC and BC mass concentrations was extracted through the standard deviation of the field blanks (Li et al., 2021). OC in snow can produce minor warming (Yasunari et al., 2015), but in this research albedo reduction from OC was not quantified. In albedo simulation and RF estimations, snow grain size and texture can produce large uncertainty. We measured/considered the physical grain size in this research, which does not have the same as the effects as optical grain size. Optical grain size defines the amount of solar radiation absorbed/scattered by the snow. We assumed a spherical shape for the snow grains, which may affect the results because the albedo of non-spherical grains is higher than the albedo of spherical grains (Dang et al., 2016; He et al., 2018). The contribution of pollutants generated from local sources can be important (Li et al., 2021), but this was not included in the global emission inventories; thus we were unable to capture emissions at the local scale. Therefore contributions of local sources may be underestimated by coarse-resolution models. High-resolution models and emission inventories at the local scale are required to capture local emissions.

6 Conclusions

The average mass concentrations of LAPs in the samples collected from the Sachin, Yala, and Thana glaciers were in the range of 835 to 3545 $ng\,g^{-1}$ for BC and 35 to 253 $\mu g\,g^{-1}$ for dust, 23 to 2529 $ng\,g^{-1}$ for BC and 1.5 to 196 $\mu g\,g^{-1}$ for dust, and 21 to 127 $ng\,g^{-1}$ for BC and 1.5 to 67 $\mu g\,g^{-1}$ for dust, respectively. Overall the concentrations of BC and dust varied from 21 $ng\,g^{-1}$ and 1.5 $\mu g\,g^{-1}$, respectively, in fresh snow to 3545 $ng\,g^{-1}$ and 253 $\mu g\,g^{-1}$, respectively, in the aged snow. Mass concentrations of BC, OC, and dust in the samples collected from the western Himalayas was much higher than the average concentration in the central Himalayas mainly due to difference in snow age, elevation, and meteorology. In the accumulation area of glaciers, the deposition of pollutants is expected to be lower, enrichment influences are less marked, and measured values are likely to be lower. Pollutant concentrations were likely underestimated in the earlier studies, particularly when there was strong surface melting. Dust and other pollutants were visible on aged-snow surfaces in the western Himalayan glacier, indicating considerable enrichment during snow aging. WRF-Chem-modeled BC concentrations in surface snow were similar to the observed BC in the snow with a smaller magnitude.

Based on observed pollutants, snow albedo reduction (%) in the central Himalayas was in the range of 0.48 %–3.6 % for BC and 0.13 %–1.99 % for dust, much lower than that of the western Himalayas. BC was the major component responsible for the albedo reduction, and the dust had little effect except at the Thana glacier. In the case of the Thana glacier, the impact of dust was higher than that of BC. The daytime instantaneous radiative forcing ($W\,m^{-2}$) ranged from 0.076 to 39.65 (Yala glacier during May 2016), 0.006 to 18.26 (Yala glacier during September 2016), 0.0 to 11.48 (Thana glacier during September 2016), and 0.03 to 96.48 (Sachin glacier during May 2016). The average albedo reduction due to the combined effect of dust and BC on the western Himalayan side (Sachin glacier) was 0.372, which was ∼ 15 times higher than that of the central Himalayan part (Yala glacier). Similarly, the radiative forcing in the western Hi-

malayas was ∼ 6 times higher than that of the central Himalayan part. Observation showed that the potential source regions of pollutants for the western and central Himalayas were different. Western Himalayan glaciers were mostly affected by long-range transport via the westerlies; however central Himalayan glaciers were affected by relatively local winds from Nepal, Bhutan, India, and China. For the western Himalayan glaciers, the emissions from central Asian and south Asian countries (particularly Pakistan and India) are more important source regions.

References

Bolch, T., Kulkarni, a., Kaab, a., Huggel, C., Paul, F., Cogley, J. G., Frey, H., Kargel, J. S., Fujita, K., Scheel, M., Bajracharya, S., and Stoffel, M.: The State and Fate of Himalayan Glaciers, Science, 336, 310–314, https://doi.org/10.1126/science.1215828, 2012.

Bond, T. C., Doherty, S. J., Fahey, D. W., Forster, P. M., Berntsen, T., Deangelo, B. J., Flanner, M. G., Ghan, S., K??rcher, B., Koch, D., Kinne, S., Kondo, Y., Quinn, P. K., Sarofim, M. C., Schultz, M. G., Schulz, M., Venkataraman, C., Zhang, H., Zhang, S., Bellouin, N., Guttikunda, S. K., Hopke, P. K., Jacobson, M. Z., Kaiser, J. W., Klimont, Z., Lohmann, U., Schwarz, J. P., Shindell, D., Storelvmo, T., Warren, S. G., and Zender, C. S.: Bounding the role of black carbon in the climate system: A scientific assessment, J. Geophys. Res.-Atmos., 118, 5380–5552, https://doi.org/10.1002/jgrd.50171, 2013.

Chow, J. C., Watson, J. G., Pritchett, L. C., Pierson, W. R., Frazier, C. A., and Purcell, R. G.: The dri thermal/optical reflectance carbon analysis system: description, evaluation and applications in U.S. Air quality studies, Atmos. Environ., 27, 1185–1201, https://doi.org/10.1016/0960-1686(93)90245-T, 1993.

Dang, C., Fu, Q., and Warren, S. G.: Effect of snow grain shape on snow albedo, J. Atmos. Sci., 73, 3573–3583, https://doi.org/10.1175/JAS-D-15-0276.1, 2016.

Dang, C., Zender, C. S., and Flanner, M. G.: Intercomparison and improvement of two-stream shortwave radiative transfer schemes in Earth system models for a unified treatment of cryospheric surfaces, The Cryosphere, 13, 2325–2343, https://doi.org/10.5194/tc-13-2325-2019, 2019.

Flanner, M. G. and Zender, C. S.: Linking snowpack microphysics and albedo evolution, J. Geophys. Res.-Atmos., 111, 1–12, https://doi.org/10.1029/2005JD006834, 2006.

Flanner, M. G., Zender, C. S., Randerson, J. T., and Rasch, P. J.: Present-day climate forcing and response from black carbon in snow, J. Geophys. Res.-Atmos., 112, 1–17, https://doi.org/10.1029/2006JD008003, 2007.

Flanner, M. G., Zender, C. S., Hess, P. G., Mahowald, N. M., Painter, T. H., Ramanathan, V., and Rasch, P. J.: Springtime warming and reduced snow cover from carbonaceous particles, Atmos. Chem. Phys., 9, 2481–2497, https://doi.org/10.5194/acp-9-2481-2009, 2009.

Grell, G. A., Peckham, S. E., Schmitz, R., McKeen, S. A., Frost, G., Skamarock, W. C., and Eder, B.: Fully coupled chem-

istry within the WRF model, Atmos. Environ., 39, 6957–6975, https://doi.org/10.1016/j.atmosenv.2005.04.027, 2005.

Gul, C., Puppala, S. P., Kang, S., Adhikary, B., Zhang, Y., Ali, S., Li, Y., and Li, X.: Concentrations and source regions of light-absorbing particles in snow/ice in northern Pakistan and their impact on snow albedo, Atmos. Chem. Phys., 18, 4981–5000, https://doi.org/10.5194/acp-18-4981-2018, 2018.

Gul, C., Mahapatra, P. S., Kang, S., Singh, P. K., Wu, X., He, C., Kumar, R., Rai, M., Xu, Y., and Puppala, S. P.: Black carbon concentration in the central Himalayas: Impact on glacier melt and potential source contribution, Environ. Pollut., 275, 116544, https://doi.org/10.1016/j.envpol.2021.116544, 2021.

Hansen, J. and Nazarenko, L.: Soot climate forcing via snow and ice albedos, P. Natl. Acad. Sci. USA, 101, 423–428, https://doi.org/10.1073/pnas.2237157100, 2004.

Hansen, J., Sato, M., and Ruedy, R.: Radiative forcing and climate response, J. Geophys. Res.-Atmos., 102, 6831–6864, https://doi.org/10.1029/96JD03436, 1997.

He, C. and Flanner, M. G.: Snow Albedo and Radiative Transfer: Theory, Modeling, and Parameterization, https://doi.org/10.1007/978-3-030-38696-2_3, 2020.

He, C., Takano, Y., Liou, K. N., Yang, P., Li, Q., and Chen, F.: Impact of snow grain shape and black carbon-snow internal mixing on snow optical properties: Parameterizations for climate models, J. Climate, 30, 10019–10036, https://doi.org/10.1175/JCLI-D-17-0300.1, 2017.

He, C., Flanner, M. G., Chen, F., Barlage, M., Liou, K.-N., Kang, S., Ming, J., and Qian, Y.: Black carbon-induced snow albedo reduction over the Tibetan Plateau: uncertainties from snow grain shape and aerosol–snow mixing state based on an updated SNICAR model, Atmos. Chem. Phys., 18, 11507–11527, https://doi.org/10.5194/acp-18-11507-2018, 2018.

Hersbach, H., Bell, B., Berrisford, P., Biavati, G., Horányi, A., Muñoz Sabater, J., Nicolas, J., Peubey, C., Radu, R., Rozum, I., et al.: ERA5 monthly averaged data on single levels from 1979 to present, [data set], Copernicus Clim. Chang. Serv. Clim. Data Store, 10, 252–266, https://doi.org/10.24381/cds.f17050d7, 2019,

Hock, R.: Glacier melt: A review of processes and their modelling, Prog. Phys. Geogr., 29, 362–391, https://doi.org/10.1191/0309133305pp453ra, 2005.

Immerzeel, W. W., van Beek, L. P. H., and Bierkens, M. F. P.: Climate change will affect the Asian water towers., Science, 328, 1382–1385, https://doi.org/10.1126/science.1183188, 2010.

Ji, Z., Kang, S., Cong, Z., Zhang, Q., and Yao, T.: Simulation of carbonaceous aerosols over the Third Pole and adjacent regions: distribution, transportation, deposition, and climatic effects, Clim. Dynam., 45, 2831–2846, https://doi.org/10.1007/s00382-015-2509-1, 2015.

Kang, S., Xu, Y., Q. You, Flügel, W., Pepin, N., and Yao, T.: Review of climate and cryospheric change in the Tibetan Plateau, Environ. Res. Lett., 5, 1–8, https://doi.org/10.1088/1748-9326/5/1/015101, 2010.

Kang, S., Zhang, Q., Qian, Y., Ji, Z., Li, C., Cong, Z., Zhang, Y., Guo, J., Du, W., Huang, J., You, Q., Panday, A. K., Rupakheti, M., Chen, D., Gustafsson, Ö., Thiemens, M. H., and Qin, D.: Linking atmospheric pollution to cryospheric change in the Third Pole region: current progress and future prospects, Nat. Sci. Rev., 6, 796–809, https://doi.org/10.1093/nsr/nwz031, 2019.

Kang, S., Zhang, Y., Qian, Y., and Wang, H.: A review of black carbon in snow and ice and its impact on the cryosphere, Earth-Sci. Rev., 210, 103346, https://doi.org/10.1016/j.earscirev.2020.103346, 2020.

Kaspari, S., Painter, T. H., Gysel, M., Skiles, S. M., and Schwikowski, M.: Seasonal and elevational variations of black carbon and dust in snow and ice in the Solu-Khumbu, Nepal and estimated radiative forcings, Atmos. Chem. Phys., 14, 8089–8103, https://doi.org/10.5194/acp-14-8089-2014, 2014.

Knote, C., Hodzic, A., Jimenez, J. L., Volkamer, R., Orlando, J. J., Baidar, S., Brioude, J., Fast, J., Gentner, D. R., Goldstein, A. H., Hayes, P. L., Knighton, W. B., Oetjen, H., Setyan, A., Stark, H., Thalman, R., Tyndall, G., Washenfelder, R., Waxman, E., and Zhang, Q.: Simulation of semi-explicit mechanisms of SOA formation from glyoxal in aerosol in a 3-D model, Atmos. Chem. Phys., 14, 6213–6239, https://doi.org/10.5194/acp-14-6213-2014, 2014.

Kumar, R., Naja, M., Satheesh, S. K., Ojha, N., Joshi, H., Sarangi, T., Pant, P., Dumka, U. C., Hegde, P., and Venkataramani, S.: Influences of the springtime northern Indian biomass burning over the central Himalayas, J. Geophys. Res.-Atmos., 116, 1–14, https://doi.org/10.1029/2010JD015509, 2011.

Kumar, R., Barth, M. C., Nair, V. S., Pfister, G. G., Suresh Babu, S., Satheesh, S. K., Krishna Moorthy, K., Carmichael, G. R., Lu, Z., and Streets, D. G.: Sources of black carbon aerosols in South Asia and surrounding regions during the Integrated Campaign for Aerosols, Gases and Radiation Budget (ICARB), Atmos. Chem. Phys., 15, 5415–5428, https://doi.org/10.5194/acp-15-5415-2015, 2015.

Li, C., Bosch, C., Kang, S., Andersson, A., Chen, P., Zhang, Q., Cong, Z., Chen, B., Qin, D., and Gustafsson, Ö.: Sources of black carbon to the Himalayan-Tibetan Plateau glaciers, Nat. Commun., 7, 1–7, https://doi.org/10.1038/ncomms12574, 2016.

Li, C., Yan, F., Kang, S., Yan, C., Hu, Z., Chen, P., Gao, S., Zhang, C., He, C., Kaspari, S., and Stubbins, A.: Carbonaceous matter in the atmosphere and glaciers of the Himalayas and the Tibetan plateau: An investigative review, Environ. Int., 146, 106281, https://doi.org/10.1016/j.envint.2020.106281, 2021.

Li, X., Kang, S., He, X., Qu, B., Tripathee, L., Jing, Z., Paudyal, R., Li, Y., Zhang, Y., Yan, F., Li, G., and Li, C.: Light-absorbing impurities accelerate glacier melt in the Central Tibetan Plateau, Sci. Total Environ., 587, 482–490, https://doi.org/10.1016/j.scitotenv.2017.02.169, 2017.

Li, Y., Chen, J., Kang, S., Li, C., Qu, B., Tripathee, L., Yan, F., Zhang, Y., Guo, J., Gul, C., and Qin, X.: Impacts of black carbon and mineral dust on radiative forcing and glacier melting during summer in the Qilian Mountains, northeastern Tibetan Plateau, The Cryosphere Discuss. [preprint], https://doi.org/10.5194/tc-2016-32, 2016.

Marcovecchio, A., Behrangi, A., Dong, X., Xi, B., and Huang, Y.: Precipitation Influence on and Response to Early and Late Arctic Sea Ice Melt Onset During Melt Season, Int. J. Clim., 42, 81–96, https://doi.org/10.1002/joc.7233, 2021.

Mayer, C., Lambrecht, A., Belò, M., Smiraglia, C., and Diolaiuti, G.: Glaciological characteristics of the ablation zone of Baltoro glacier, Karakoram, Pakistan, Ann. Glaciol., 43, 123–131, https://doi.org/10.3189/172756406781812087, 2006.

Ming, J., Xiao, C., Cachier, H., Qin, D., Qin, X., Li, Z., and Pu, J.: Black Carbon (BC) in the snow of glaciers in west China

and its potential effects on albedos, Atmos. Res., 92, 114–123, https://doi.org/10.1016/j.atmosres.2008.09.007, 2009.

Niu, H., Kang, S., Wang, Y., Sarangi, C., Rupakheti, D., and Qian, Y.: Measurements of light-absorbing impurities in snow over four glaciers on the Tibetan Plateau, Atmos. Res., 243, ISSN 0169-8095, https://doi.org/10.1016/j.atmosres.2020.105002, 2020.

Pepin, N. C., and Lundquist, J. D.: Temperature trends at high elevations: Patterns across the globe, Geophys. Res. Lett., 35, 1–6, https://doi.org/10.1029/2008GL034026, 2008.

Qian, Y., Flanner, M. G., Leung, L. R., and Wang, W.: Sensitivity studies on the impacts of Tibetan Plateau snowpack pollution on the Asian hydrological cycle and monsoon climate, Atmos. Chem. Phys., 11, 1929–1948, https://doi.org/10.5194/acp-11-1929-2011, 2011.

Qian, Y., Wang, H., Zhang, R., Flanner, M. G., and Rasch, P. J.: A sensitivity study on modeling black carbon in snow and its radiative forcing over the Arctic and Northern China, Environ. Res. Lett., 9, 64001, https://doi.org/10.1088/1748-9326/9/6/064001, 2014.

Qu, B., Ming, J., Kang, S.-C., Zhang, G.-S., Li, Y.-W., Li, C.-D., Zhao, S.-Y., Ji, Z.-M., and Cao, J.-J.: The decreasing albedo of the Zhadang glacier on western Nyainqentanglha and the role of light-absorbing impurities, Atmos. Chem. Phys., 14, 11117–11128, https://doi.org/10.5194/acp-14-11117-2014, 2014.

Quinn, P. K., Bates, T. S., Baum, E., Doubleday, N., Fiore, A. M., Flanner, M., Fridlind, A., Garrett, T. J., Koch, D., Menon, S., Shindell, D., Stohl, A., and Warren, S. G.: Short-lived pollutants in the Arctic: their climate impact and possible mitigation strategies, Atmos. Chem. Phys., 8, 1723–1735, https://doi.org/10.5194/acp-8-1723-2008, 2008.

Rai, M., Mahapatra, P. S., Gul, C., Kayastha, R. B., Panday, A. K., and Puppala, S. P.: Aerosol Radiative Forcing Estimation over a Remote High-altitude Location (∼ 4900 m a.s.l.) near Yala Glacier, Nepal, Aerosol Air Qual. Res., 19, 1872–1891, https://doi.org/10.4209/aaqr.2018.09.0342, 2019.

Ramanathan, V. and Carmichael, G.: Global and regional climate changes due to black carbon, Nat. Geosci., 1, 221–227, https://doi.org/10.1038/ngeo156, 2008.

Ricchiazzi, P., Yang, S. R., Gautier, C., and Sowle, D.: SB DART: A Research and Teaching Software Tool for Plane-Parallel Radiative Transfer in the Earth's Atmosphere, B. Am. Meteorol. Soc., 79, 2101–2114, 1998.

Schmale, J., Flanner, M., Kang, S., Sprenger, M., Zhang, Q., Guo, J., Li, Y., Schwikowski, M., and Farinotti, D.: Modulation of snow reflectance and snowmelt from Central Asian glaciers by anthropogenic black carbon, Sci. Rep., 7, ISSN 2045-2322, https://doi.org/10.1038/srep40501, 2017.

Tripathee, L., Gul, C., Kang, S., Chen, P., Huang, J., and Rai, M.: Transport Mechanisms, Potential Sources, and Radiative Impacts of Black Carbon Aerosols on the Himalayas and Tibetan Plateau Glaciers, in: Air Pollution and Its Complications: From the Regional to the Global Scale, edited by: Tiwari, S. and Saxena, P., Springer International Publishing, Cham, 7–23, https://doi.org/10.1007/978-3-030-70509-1_2, 2021.

Vaux, H. J., Balk, D., Gleick, P., William, K. M. Lau., Levy, M., Malone, L. E., Mcdonald, R., Shindell, D., Thompson, G. L., Wescoat, L. J., and Williams, W. M.: Himalayan Glaciers: Climate Change, Water Resources, and Water Security, The National Academies Press, National Academies Press, Washington,

DC, ISSN 0-309-26098-1 pp., https://doi.org/10.17226/13449, 2012.

Wang, X., Pu, W., Ren, Y., Zhang, X., Zhang, X., Shi, J., Jin, H., Dai, M., and Chen, Q.: Observations and model simulations of snow albedo reduction in seasonal snow due to insoluble light-absorbing particles during 2014 Chinese survey, Atmos. Chem. Phys., 17, 2279–2296, https://doi.org/10.5194/acp-17-2279-2017, 2017.

Wang, Y., Ma, P. L., Peng, J., Zhang, R., Jiang, J. H., Easter, R. C., and Yung, Y. L.: Constraining Aging Processes of Black Carbon in the Community Atmosphere Model Using Environmental Chamber Measurements, J. Adv. Model. Earth Syst., 10, 2514–2526, https://doi.org/10.1029/2018MS001387, 2018.

Warren, S. G. and Brandt, R. E.: Optical constants of ice from the ultraviolet to the microwave: A revised compilation, J. Geophys. Res.-Atmos., 113, 1–10, https://doi.org/10.1029/2007JD009744, 2008.

Xu, B., Yao, T., Liu, X., and Wang, N.: Elemental and organic carbon measurements with a two-step heating-gas chromatography system in snow samples from the Tibetan Plateau, Ann. Glaciol., 43, 257–262, https://doi.org/10.3189/172756406781812122, 2006.

Xu, B., Cao, J., Joswiak, D. R., Liu, X., Zhao, H., and He, J.: Post-depositional enrichment of black soot in snow-pack and accelerated melting of Tibetan glaciers, Environ. Res. Lett., 7, 014022, https://doi.org/10.1088/1748-9326/7/1/014022, 2012.

Yang, S., Xu, B., Cao, J., Zender, C. S., and Wang, M.: Climate effect of black carbon aerosol in a Tibetan Plateau glacier, Atmos. Environ., 111, 71–78, https://doi.org/10.1016/j.atmosenv.2015.03.016, 2015.

Yao, T., Xue, Y., Chen, D. L., Chen, F., Thompson, L. G., Cui, P., Koike, T., Lau, W. K. M., Lettenmaier, D. P., Mosbrugger, V., Zhang, R., Xu, B., Dozier, J., Gillespie, T. W., Gu, Y., Kang, S., Piao, S., Sugimoto, S., Ueno, K., Wang, L., Wang, W., Zhang, F., Sheng, Y., Guo, W., Ailikun, Yang, X., Ma, Y., Shen, S. S. P., Su, Z., Chen, F., Liang, S., Liu, Y., Singh, V. P., Yang, K., Yang, D., Zhao, X., Qian, Y., Zhang, Y., and Li, Q.: Recent Third Pole's Rapid Warming Accompanies Cryospheric Melt and Water Cycle Intensification and Interactions between Monsoon and Environment: Multidisciplinary Approach with Observations, Modeling, and Analysis, B. Am. Meteorol. Soc., 100, 423–444, 2019.

Yasunari, T. J., Bonasoni, P., Laj, P., Fujita, K., Vuillermoz, E., Marinoni, A., Cristofanelli, P., Duchi, R., Tartari, G., and Lau, K.-M.: Estimated impact of black carbon deposition during pre-monsoon season from Nepal Climate Observatory – Pyramid data and snow albedo changes over Himalayan glaciers, Atmos. Chem. Phys., 10, 6603–6615, https://doi.org/10.5194/acp-10-6603-2010, 2010.

Yasunari, T. J., Koster, R. D., Lau, W. K. M., and Kim, K.: Impact of snow darkening via dust, black carbon, and organic carbon on boreal spring climate in the Earth system, J. Geophys. Res.-Atmos., 120, 5485–5503, https://doi.org/10.1002/2014JD022977, 2015.

You, Q., Cai, Z., Pepin, N., Chen, D., Ahrens, B., Jiang, Z., Wu, F., Kang, S., Zhang, R., Wu, T., Wang, P., Li, M., Zuo, Z., Gao, Y., Zhai, P., and Zhang, Y.: Warming amplification over the Arctic Pole and Third Pole: Trends, mechanisms and consequences, Earth-Sci. Rev., 217, 103625, https://doi.org/10.1016/j.earscirev.2021.103625, 2021.

Zaveri, R. A., Easter, R. C., Fast, J. D., and Peters, L. K.: Model for Simulating Aerosol Interactions and Chemistry (MOSAIC), J. Geophys. Res.-Atmos., 113, D13204, https://doi.org/10.1029/2007JD008782, 2008.

Zhang, Q., Kang, S., Kaspari, S., Li, C., Qin, D., Mayewski, P. A., and Hou, S.: Rare earth elements in an ice core from Mt. Everest: Seasonal variations and potential sources, Atmos. Res., 94, 300–312, https://doi.org/10.1016/j.atmosres.2009.06.005, 2009.

Zhang, Y., Kang, S., Cong, Z., Schmale, J., Sprenger, M., Li, C., Yang, W., Gao, T., Sillanpää, M., Li, X., Liu, Y., Chen, P., and Zhang, X.: Light-absorbing impurities enhance glacier albedo reduction in the southeastern Tibetan plateau, J. Geophys. Res., 122, 6915–6933, https://doi.org/10.1002/2016JD026397, 2017.

Zhang, Y., Kang, S., Sprenger, M., Cong, Z., Gao, T., Li, C., Tao, S., Li, X., Zhong, X., Xu, M., Meng, W., Neupane, B., Qin, X., and Sillanpää, M.: Black carbon and mineral dust in snow cover on the Tibetan Plateau, The Cryosphere, 12, 413–431, https://doi.org/10.5194/tc-12-413-2018, 2018.

Zhao, C., Hu, Z., Qian, Y., Ruby Leung, L., Huang, J., Huang, M., Jin, J., Flanner, M. G., Zhang, R., Wang, H., Yan, H., Lu, Z., and Streets, D. G.: Simulating black carbon and dust and their radiative forcing in seasonal snow: a case study over North China with field campaign measurements, Atmos. Chem. Phys., 14, 11475–11491, https://doi.org/10.5194/acp-14-11475-2014, 2014.